AIAA Atmospheric Flight Mechanics Conference
10 - 13 August 2009, Chicago, Illinois

AIAA 2009-5707

Step-Based Experiment Design and System Identification for Aeroelastic Dynamic Modeling

Raymond A. de Callafon * and Daniel N. Miller †
University of California San Diego, La Jolla, CA 92093-0411

Jie Zeng ‡
ZONA Technology Inc., Scottsdale, AZ 85258-4578

Martin J. Brenner §
NASA Dryden Flight Research Center, Edwards, CA 93523-0273

This paper gives an overview of the main ideas behind a new estimation technique that is able to deliver a consistent estimate of (poorly-damped) structural resonance modes induced by aeroservoelastic interaction without user intervention. Instead of using broadband sinusoidal or sine-sweep excitation signals, the new estimation method proposed in this paper uses simple step-based excitation signals that can be applied to any of the control surfaces to formulate a model of the aerodynamically-induced structural vibration modes. Simple step-based excitation signals address the issue of broadband excitation while allowing a reasonable (short-time) excitation signal on the control surfaces.

The proposed estimation method has been tailored to find consistent model estimates on the basis of step-based input signals. The estimation method uses a modified version of the well-known realization algorithm that is extended to arbitrary input signals to formulate a discrete-time model directly on the basis of step-based experiments. Since the numerical implementation only requires a singular value decomposition and a standard least-squares estimation, robust numerical algorithms can be put in place to formulate a dynamical model with little or no user intervention. The procedure is illustrated on time-domain data obtained from a high fidelity model of an F/A-18 to find a low-order model that captures the structural parameters, such as damping and location of the first main resonance modes.

I. Introduction

The steady development of new sensors and weapons technology requires that engineers be able to integrate new stores configurations for existing aircraft quickly and efficiently. For modern aircraft with expansive flight envelopes, the introduction of new payloads can introduce unpredictable and undesirable changes in an aircraft's structural dynamics, and potentially dangerous resonance modes induced by aeroservoelastic interaction must be dampened by flight controller augmentation.

With available sensor technology, poorly-damped structural resonance modes induced by aeroservoelastic interaction can be monitored and modeled via data-based estimation techniques.[1–3] Such estimation techniques can use time-domain measurements of input-output behavior to formulate a dynamical model suitable for control system design. Based on the information of structural parameters captured in a dynamical model, a model-based feedback control design technique can be used to dampen the resonance modes using the flight control surfaces[4] or to predict flutter margins.[5]

A myriad of algorithms exist for the identification of models for a system that are suitable for control system design. Most common are the prediction-error methods, unified in the work of Ljung[6] and selectively

*Assoc. Prof. of Mechanical and Aerospace Engineering, callafon@ucsd.edu
†Graduate Student of Mechanical and Aerospace Engineering, Student Member AIAA, danielmiller@ucsd.edu
‡R&D control engineer, member AIAA, jzeng@zonatech.com
§Aerospace Engineer, member AIAA, martin.j.brenner@nasa.gov

applied to aerospace vehicles in Klein and Morelli[7] and Jategaonkar.[8] Alternatively, realization-based algorithms construct state-space models by estimating a subspace that contains the relevant system dynamics and then extracting system matrices from a basis of this subspace.

The most popular of these are the N4SID family of algorithms, which estimate the subspace spanned by the system's extended observability matrix by projecting the system output onto the nullspace of future input signals. These are thoroughly presented in the work by Overschee and de Moor[9,10] and the contribution by Katayama.[11] A similar algorithm that replaces the projection step with a least-squares problem was applied to the identification of aeroelastic modes in the work of Mehra and co-authors.[12]

Another realization-based identification algorithm commonly used for aerospace structures is the Eigensystem Realization Algorithm,[13] which uses either the impulse-response or the full frequency response of a system to estimate the subspace spanned by the system Hankel matrix. Estimating the frequency response or the system impulse response possibly via inverse Fourier transform typically requires broadband excitation – something that is often impractical for in-flight testing. Alternative input signals for aircraft parameter identification[14] can potentially provide improved results,[15] motivating the formulation of the estimation algorithm in this paper that is tailored to specific (step-based) input signals. Moreover, the computational algorithms of the estimation algorithm are based on stable numerical algorithms and require little or no user intervention to formulate a state-space model of a given McMillan degree.

The algorithm presented in this paper estimates the subspace spanned by the system Hankel matrix not by projecting out future input effects or estimating the impulse response directly but by analytically isolating the system Hankel matrix based on the structure of the input signal and the assumption that the system is initially at rest. The resulting algorithm provides high-quality state-space models from practical, succinct data sets generated by step-based excitation signals on control surfaces of the aircraft, allowing the estimation of possible flexible modes due to aero(servo)elastic interaction.

II. F/A-18AAW Model

II.A. Nonlinear 6-DOF Rigid-Body Flight Model of F/A-18AAW

For testing of the proposed identification methods presented in this paper, ZONA has developed a high-fidelity, nonlinear 6-DOF rigid-body simulation model of the F/A-18AAW aircraft coupled to a linear aeroelastic solver[16] to generate data for the identification algorithms. Since the emphasis of the paper lies with the actual identification algorithms, only a summary of the high fidelity model is given here.

The nonlinear 6-DOF rigid-body simulation model was developed for the Simulink environment using a set of libraries from the Aerospace Blockset of Matlab simulink software.[17] A general formulation of the aircraft flight dynamics is implemented by considering the dynamics of the rigid-body vehicle and moving component subsystems (control surfaces), subject to aerodynamic and gravitational forces.

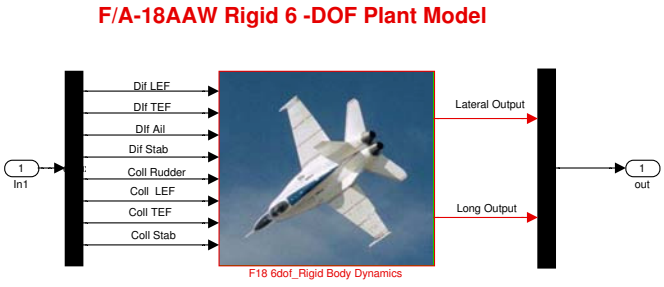

Figure 1. Open-Loop 6-DOF Nonlinear Simulation Plant Model.

The open-loop F/A-18AAW nonlinear Simulink model is depicted in Figure 1, with a selected set of input and output variables that match the actual ones used in the F/A-18AAW aircraft. The developed open-loop nonlinear model allows for fifteen longitudinal and fifteen lateral-directional dynamics output components, while five differential and three collective control commands are also defined and are summarized in Tables 1, 2 and 3, respectively. This high-fidelity, rigid-body airframe model was developed using the following elements:

1. `Six (6) Degrees-Of-Freedom` solver using Euler angles subsystem.
2. `Aerodynamic Forces and Moments` subsystem using the set of non-dimensional stability and control derivatives obtained through the set of AAW Parameter IDentification (PID) flight tests.
3. `Airflow` and `Sensors` subsystems.

Table 1. Control Input Components for the Nonlinear Simulation Model.

Lateral-Directional Effector	*Longitudinal Effector*
Differential LEF [Dif LEF] - (deg)	Collective LEF [Coll LEF] - (deg)
Differential TEF [Dif TEF] - (deg)	Collective TEF [Coll TEF] - (deg)
Differential Ail [Dif AIL] - (deg)	Collective Stab [Coll STAB] - (deg)
Differential Stab [Dif STAB] - (deg)	
Collective Rudder [Coll RUDD] - (deg)	

Table 2. Longitudinal Dynamics Output Components.

u	Body axis linear velocity	ft/s
q	Body pitch rate	deg/s
θ	Body pitch attitude	deg
$\dot{\alpha}$	Time rate of change of angle of attack	deg/s
α	Angle of attack	deg
h	Altitude	ft
$N_{Z_{cg}}$	Body normal acceleration at cg (+up)	g
$N_{Z_{sens}}$	Body normal acceleration at accelerometer (+ up)	g
$N_{X_{cg}}$	Body axial acceleration (+ forward)	g
$N_{Z_{plt}}$	Body normal acceleration at cockpit (+ up)	g
$\dot{u}$	Time rate of change of body linear velocity	ft/s^2
$\dot{q}$	Body pitch angular acceleration	deg/s^2

The open-loop nonlinear rigid-body 6-DOF flight dynamics model is integrated with a generic flight control law synthesized for operating conditions of Mach = 0.9 and Altitude = 15K ft. Linear models and controllers representative of the actual aircraft were used to test closed-loop simulation of the F/A18-AAW Simulink model. The related gains and architecture for the flight control law were validated by comparing closed-loop results from the F/A-18 AAW nonlinear model as well as from the linearized F/A-18 C/D model. Closed-loop responses from our high-fidelity nonlinear F/A-18 AAW model were consistent with the ones obtained from the F/A-18 C/D aircraft.

II.B. Linear Aeroelastic Solver

To provide a unified formulation for the aeroelastic interaction between a flexible structure and its airflow, a model for a flexible aircraft is defined with respect to a body-fixed reference system and driven by aerodynamic, thrust, elastic and gravity (g) forces and moments. The model was also developed and implemented in the `Matlab/Simulink` simulation environment where the nonlinear flight dynamics are defined as:

$$m\left[\dot{V}_b + \Omega_b \times V_b - R_{bg}(E)\,[0,\,0,\,g]^T\right] \;=\; F_A + F_\delta + F_T + \Delta_F$$

$$J\dot{\Omega}_b + \Omega_b \times J\Omega_b \;=\; M_A + M_\delta + M_T + \Delta_M$$

where m and J are the air vehicle mass and inertia tensor, and $R_{bg}(E)$ is the rotation mapping from inertial to body-axes, ($E = [\,\phi,\ \theta,\ \psi\,]$). The dynamics described above are driven by the forces and moments on the

Table 3. Lateral-Directional Dynamics Output Components.

β	Sideslip angle	rad
p	Body axis roll rate	rad/s
r	Body axis yaw rate	rad/s
ϕ	Body roll attitude	rad
ψ	Body yaw attitude	rad
$N_{Y_{cg}}$	Body lateral acceleration at cg	g
$N_{Y_{sens}}$	Body lateral acceleration at accelerometer	g
p_{sens}	Body axis roll rate	rad/s
r_{sens}	Body axis yaw rate	rad/s
$\dot{\beta}$	Time rate of change of sideslip angle	rad/s
$\dot{p}$	Body axis roll angular acceleration	rad/s^2
$\dot{r}$	Body axis yaw angular acceleration	rad/s^2

right-hand side. Here, F_A and M_A are the external aerodynamic forces and moments on the air vehicle. They are a function of the aerodynamic flight states, Mach number, body angular rates (Ω_b) and control surface deflections and are usually obtained by CFD computations, wind-tunnel data, or flight tests. F_δ and M_δ are the aerodynamic forces and moments from the control surfaces commanded by the flight control system and pilot inputs while F_T and M_T includes the thrust loads. Δ_F and Δ_M are the aeroelastic incremental loads due to the structural oscillation and are computed by an incremental aeroelastic forces and moments solver.[16]

This incremental aeroelastic forces and moments solver is a state space equation whose state are the modal coordinates of the elastic modes, defined here as η_e, and the aerodynamic lags. The input of the incremental aeroelastic forces and moments solver is the incremental airframe state and the incremental control input provided by the rigid-body 6-DOF flight dynamic model and the output is the incremental forces and moments due to the aeroelastic effects, ΔF and ΔM, that are added to the 6-DOF equation of motion. In addition, the incremental aeroelastic forces and moments solver compute the effects of structure dynamics at the sensor locations. These effects are added to the sensor output of the rigid-body motion. Note that the aerodynamic lags are introduced by the rational function approximation of the frequency domain unsteady aerodynamics computed by the unsteady aerodynamic methods.[18]

The linear aeroelastic solver was built into the Simulink block diagram depicted in Figure 2. It can be seen that the `Incremental Aeroelastic Forces and Moments Solver` is interconnected with the `F/A-18AAW Rigid 6-DOF` subsystem throughout the input vectors denoted as *Effectors* and *Airframe States* and output vectors denoted as Δ_F, Δ_M, and η_e.

III. Preliminaries

Consider a discrete, linear, time-invariant system described in state-space form as

$$\begin{aligned} x(t+1) &= Ax(t) + Bu(t) \\ y(t) &= Cx(t) + Du(t) + v(t) \end{aligned} \tag{1}$$

with state vector $x \in \mathbb{R}^n$, input vector $u \in \mathbb{R}^m$, output vector $y \in \mathbb{R}^p$, and system matrices $A \in \mathbb{R}^{n\times n}$, $B \in \mathbb{R}^{n\times m}$, $C \in \mathbb{R}^{p\times n}$, $D \in \mathbb{R}^{p\times m}$. The vector $v \in \mathbb{R}^p$ is a zero-mean, possibly-colored noise signal with constant variance that is uncorrelated with the input u. We restrict ourselves to systems that are both controllable and observable.

The input-output map can alternatively be described by the convolution operation

$$y(t) = \sum_{k=0}^{\infty} g(k)u(t-k) + v(t) \tag{2}$$

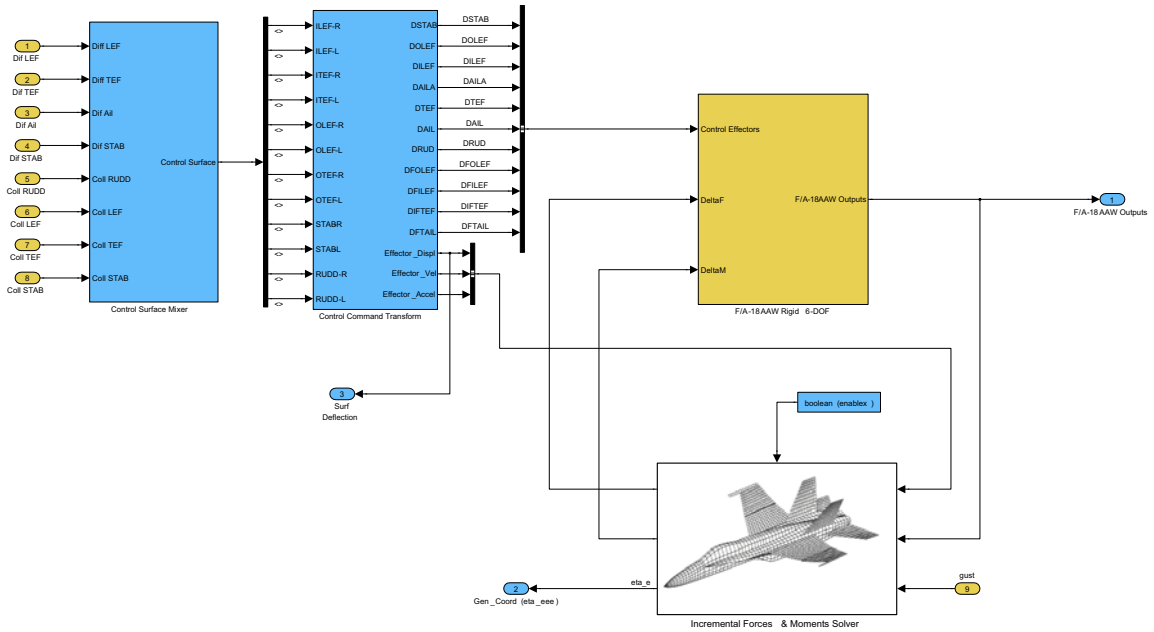

Figure 2. Addition of the Incremental Aeroelastic Forces and Moments Solver to the Nonlinear Rigid-Body 6-DOF Subsystem.

involving the system Markov parameters $g(k)$ defined as

$$g(k) = \begin{cases} D & k = 0 \\ CA^{k-1}B & k > 0 \end{cases}. \tag{3}$$

When applied to sequences of input-output data, (2) may be expressed with two matrices mapping past and future input sequences, u_p and u_f respectively, onto a future output sequence y_f, as

$$y_f = Hu_p + Tu_f + v \tag{4}$$

in which

$$\begin{aligned} u_p &= \begin{bmatrix} u(0) & u(-1) & u(-2) & \cdots \end{bmatrix}^T, \\ u_f &= \begin{bmatrix} u(1) & u(2) & u(3) & \cdots \end{bmatrix}^T, \\ y_f &= \begin{bmatrix} y(1) & y(2) & y(3) & \cdots \end{bmatrix}^T, \\ v &= \begin{bmatrix} v(1) & v(2) & v(3) & \cdots \end{bmatrix}^T, \end{aligned}$$

and

$$H = \begin{bmatrix} g(1) & g(2) & \cdots \\ g(2) & g(3) & \cdots \\ \vdots & \vdots & \ddots \end{bmatrix}, \; T = \begin{bmatrix} g(0) & & 0 \\ g(1) & g(0) & \\ \vdots & \vdots & \ddots \end{bmatrix}.$$

T is a block-Toeplitz matrix of Markov parameters, which maps all future input data $\{u(t)|t \geq 1\}$ onto future output data $\{y(t)|t \geq 1\}$, and H is a block-Hankel matrix of system Markov parameters, which maps all past input $\{u(t)|t < 1\}$ onto future output. The state of the system at time $t = 1$ is thus determined by the term Hu_p.

Examining (4), the linearity and time-invariance of the system leads to the following observations:

- Sequences of data generated by the system can be expressed as linear combinations of other sequences of data generated by the same system.
- A sufficient number of linearly-independent data sequences of a given length will contain a basis for the subspace containing all sequences of the same length that can be generated by the system.

The goal of realization-based identification algorithms is to find a system realization from a factorization of this basis.

IV. Impulse-Based Realization

The objective of the impulse-based deterministic realization problem is to find the system order n and a state-space model (1) with respect to an arbitrary state basis given a finite number of system Markov parameters (2). A celebrated algorithm given by[19] uses the following two facts to obtain the system matrices (A, B, C) from the Hankel matrix H filled with Markov parameters:

1. H is the product of the extended observability matrix Γ and the extended controllability matrix Ω:

$$H = \Gamma\Omega = \begin{bmatrix} C & CA & CA^2 & \cdots \end{bmatrix}^T \begin{bmatrix} B & AB & A^2B & \cdots \end{bmatrix}.$$

2. H exhibits a *shift-invariant* property such that should H be shifted up by p rows or to the left by m rows, the result is a block-Hankel matrix $\overrightarrow{H}$ with the property

$$\overrightarrow{H} = \Gamma A \Omega.$$

A controllable and observable system implies that Γ and Ω respectively have full column and full row rank n, making H a rank-n matrix. Thus, given a finite-dimensional pair $H \in \mathbb{R}^{N_1 \times N_2}$ and $\overrightarrow{H} \in \mathbb{R}^{N_1 \times N_2}$

$$\begin{aligned} H &= \begin{bmatrix} g(1) & g(2) & \cdots & g(n_2) \\ g(2) & g(3) & \cdots & g(n_2+1) \\ \vdots & \vdots & \ddots & \vdots \\ g(n_1) & g(n_1+1) & \cdots & g(n_1+n_2-1) \end{bmatrix} \\ \overrightarrow{H} &= \begin{bmatrix} g(2) & g(3) & \cdots & g(n_2+1) \\ g(3) & g(4) & \cdots & g(n_2+2) \\ \vdots & \vdots & \ddots & \vdots \\ g(n_1+1) & g(n_1+2) & \cdots & g(n_1+n_2) \end{bmatrix} \end{aligned} \tag{5}$$

in which $N_1 = n_1 \cdot p \geq n$ and $N_2 = n_2 \cdot m \geq n$, for any factorization of H

$$\begin{aligned} H &= \Gamma\Omega \\ &= \begin{bmatrix} C & CA & \cdots & CA^{n_1-1} \end{bmatrix}^T \begin{bmatrix} B & AB & \cdots & A^{n_2-1}B \end{bmatrix} \end{aligned}$$

there exist a left inverse $\Gamma^\dagger$ of Γ and a right inverse $\Omega^\dagger$ of Ω such that A may be solved for as

$$A = \Gamma^\dagger \overrightarrow{H} \Omega^\dagger. \tag{6}$$

$(\cdot)^\dagger$ denotes the Moore-Penrose psuedoinverse. C is subsequently taken as the first p rows of Γ and B from the first m columns of Ω. With D taken from $g(0)$, a complete, irreducible, state-space realization of (1) is obtained.

Although the use of impulse-based signals on control surfaces provide broadband excitation for identification purposes, the usage of such signals is highly unrealistic. In the following we show how such broadband excitation signals can be avoided and replaced by more realistic step-based excitation signals.

V. Step-Based Realization

V.A. Data-Matrix Equations

To formulate similar realization-based algorithms on the basis of step-based excitation signals is to first quantify a basis for the subspace that allows us to reconstruct a state-space model. To stay with the familiar realization algorithm as defined above, it will be the subspace spanned by the system Hankel matrix H. For a persistently exciting input signal, linear-indepence of data sequences can be attained by windowing a single, longer data sequence and organizing the smaller sequences into a Hankel matrix.[10] By forming a Hankel matrix of future output data

$$Y_f = \begin{bmatrix} y(1) & y(2) & \cdots & y(n_2) \\ y(2) & y(3) & \cdots & y(n_2+1) \\ \vdots & \vdots & \ddots & \vdots \\ y(n_1) & y(n_1+1) & \cdots & y(n_1+n_2-1) \end{bmatrix}, \tag{7}$$

a Hankel matrix of future input data

$$U_f = \begin{bmatrix} u(1) & u(2) & \cdots & u(n_2) \\ u(2) & u(3) & \cdots & u(n_2+1) \\ \vdots & \vdots & \ddots & \vdots \\ u(n_1+1) & u(n_1+2) & \cdots & u(n_1+n_2) \end{bmatrix},$$

and a Hankel matrix of noise data

$$V = \begin{bmatrix} v(1) & v(2) & \cdots & v(n_2) \\ v(2) & v(3) & \cdots & v(n_2+1) \\ \vdots & \vdots & \ddots & \vdots \\ v(n_1) & v(n_1+1) & \cdots & v(n_1+n_2-1) \end{bmatrix},$$

the data can be expressed in a matrix form as

$$Y_f = HU_p + TU_f + V \tag{8}$$

in which the matrix U_p is a Toeplitz matrix of past input values. If the system is initially at rest, this matrix is square and of finite dimensions:

$$U_p = \begin{bmatrix} u(0) & u(1) & \cdots & u(n_2-1) \\ 0 & u(0) & \cdots & u(n_2-2) \\ \vdots & \vdots & \ddots & \vdots \\ 0 & 0 & \cdots & u(0) \end{bmatrix}.$$

The shift-invariance of the Hankel matrices in (5) can be extended to the measured output matrix Y_f. Defining $\overrightarrow{Y}_f$ as Y_f shifted by a single column to the left, thus now including $y(N)$ $(N = n_1 + n_2)$ yields

$$\overrightarrow{Y}_f = \begin{bmatrix} y(2) & y(3) & \cdots & y(n_2+1) \\ y(3) & y(4) & \cdots & y(n_2+2) \\ \vdots & \vdots & \vdots & \vdots \\ y(n_1+1) & y(n_1+2) & \cdots & y(n_1+n_2) \end{bmatrix}.$$

and the resulting column-wise shift allows one to write a shifted data equation

$$\overrightarrow{Y}_f = \overrightarrow{H}U_p + \overrightarrow{T}U_f + \overrightarrow{V} \tag{9}$$

where $\overrightarrow{H}$ is given in (5) and

$$\overrightarrow{T} = \begin{bmatrix} g(1) & g(0) & 0 & \cdots & 0 \\ g(2) & g(1) & g(0) & \cdots & 0 \\ \vdots & \vdots & \vdots & \vdots & \vdots \\ g(N_1) & g(N_1-1) & \cdots & g(1) & g(0) \end{bmatrix}, \quad \overrightarrow{\Gamma} = \begin{bmatrix} CA \\ \vdots \\ CA^{n_1} \end{bmatrix}.$$

The data equation given in (8) and the shifted data equation in (9) form the basis of the step-based identification algorithm.

V.B. Identification from Step-Based Experiments

Instead of applying a unit-pulse excitation signal, consider the more practical situation of applying a unit-step input with initial state $x_0 = 0$. The matrix U_p is then an upper-triangular unity matrix, and the matrix product TU_f is given by

$$TU_f = \begin{bmatrix} g(0) & g(0) & \cdots & g(0) \\ g(0)+g(1) & g(0)+g(1) & \cdots & g(0)+g(1) \\ \vdots & \vdots & & \vdots \\ \sum_{i=0}^{L} g(i) & \sum_{i=0}^{L} g(i) & \cdots & \sum_{i=0}^{L} g(i) \end{bmatrix}$$

which is equivalent to the noise-free step response data

$$TU_f = \begin{bmatrix} y(0) & y(0) & \cdots & y(0) \\ y(1) & y(1) & \cdots & y(1) \\ \vdots & \vdots & & \vdots \\ y(L) & y(L) & \cdots & y(L) \end{bmatrix} \tag{10}$$

In the deterministic case, the *weighted* Hankel matrix $R = HU_p$ can be computed from (8) via

$$R = HU_p = Y_f - TU_f$$

where Y_f is simply a Hankel matrix (7) with step output response measurements and the product TU_f given in (10) is a matrix with identical columns filled with step output response measurements. A similar shifted version $\overrightarrow{R}$ can be computed from (9).[20] The following results hold for R and $\overrightarrow{R}$ in the deterministic case:

- If $u(0) \neq 0$, the square $N_2 \times N_2$ matrix U_p has full rank. Consequently, $\text{rank}(R) = \text{rank}(H) = n$, and R has a decomposition $R = R_1 R_2$ in which R_1 and R_2 have respectively full column rank n and full row rank n. In the case of noise-corrupted observations, a rank-n approximation of R can be found via its SVD.
- Since $R = HU_p$ is a post-multiplication of H, R exhibits the same shift-invariant property as H, and therefore $\overrightarrow{R} = R_1 A R_2$ can be used to recover A via left and right inverses taken from the decomposition $R = R_1 R_2$.

The above observations imply that a realization algorithm similar to Kung's can be formulated using R instead of H. Given the output $y(t)$ of a unit-step response, applying the realization algorithm to $R = Y_f - TU_f$ will yield significantly better results than applying the algorithm to an estimate of H obtained by *differentiating* the step response measurements, as doing so would amplify high-frequency noise and increase the variance of the estimated parameters.

V.C. Realization from Noise-Corrupted Measurements

If imperfect measurements of the step response in the Hankel matrix R are used to create a noise-perturbed matrix $\hat{R}$, non-deterministic effects will likely cause $\hat{R}$ to have full rank regardless of its dimensions. This

would imply that the system has infinite order, making a state-space realization impossible. To address this, the dimension of the subspace is reduced via a model-reduction problem so that only the most significant parts of $\hat{R}$ are retained. As in,[21] both the system order n and a rank-n estimate of the Hankel matrix R can be computed from the singular-value decomposition (SVD) of $\hat{R}$:

$$\hat{R} = \begin{bmatrix} U_n & U_s \end{bmatrix} \begin{bmatrix} \Sigma_n & 0 \\ 0 & \Sigma_s \end{bmatrix} \begin{bmatrix} V_n^T \\ V_s^T \end{bmatrix}$$

in which Σ_n and Σ_s are diagonal matrices containing the singular values ordered from largest to smallest, such that the first n singular values of $\hat{H}$ are contained in Σ_n and the remaining in Σ_s.

In the deterministic case, $\hat{R} = R$, $\text{rank}(\hat{R}) = n$, and $\Sigma_s = 0$. In the non-deterministic case, a "large" $\hat{R}$ will exhibit a relatively large difference in the value between the n^{th} and the $(n+1)^{\text{th}}$ singular value. An estimate of n may be determined by choosing a threshold at which the singular values decrease significantly, and a rank-n approximation of $\hat{R}$ is then given by

$$\hat{R}_n = U_n \Sigma_n V_n^T. \tag{11}$$

The decomposition of $\hat{R}_n$ in (11) also provides a convenient means of factoring the controllability and observability matrices as

$$\Gamma = U_n \Sigma_n^{1/2}, \qquad \Omega = \Sigma_n^{1/2} V_n^T,$$

with the expressions for the left inverse $\Gamma^\dagger$ and right inverse $\Omega^\dagger$ in (6) simplifying to

$$\Gamma^\dagger = \Sigma_n^{-1/2} U_n^T, \qquad \Omega^\dagger = V_n \Sigma_n^{-1/2}.$$

allowing the A-matrix of the state space realization to be estimated via

$$\hat{A} = \Gamma^\dagger \overrightarrow{H} \Omega^\dagger$$

An estimate $\hat{B}$ of the input matrix B is subsequently taken as the first m columns of Ω. With the estimates $\hat{A}$ and $\hat{B}$ known, the state vector $x(t)$ may be reconstructed via the recursive formula

$$\hat{x}(t+1) = \hat{A}\hat{x}(t) + \hat{B}u(t), \ x(0) = 0$$

for $t = 0, 1, \ldots, N$. With the reconstructed state vector $\hat{x}(t)$, the realization algorithm that is used to compute the $\hat{A}$ and $\hat{B}$ matrices, can be followed by a standard least-squares optimization problem to compute an estimate $\hat{C}$ of the output matrix C and an estimate $\hat{D}$ of the (possible) feedthrough matrix D.

Using the reconstructed state $\hat{x}(t)$, a least-squares problem can be used to estimate (any of) the state matrices by rewriting (1) into

$$Y(t) = \Theta U(t) + V(t), \ t = 1, \ldots, N$$

where

$$Y(t) = \begin{bmatrix} \hat{x}(t+1) \\ y(t) \end{bmatrix}, \ \Theta = \begin{bmatrix} \hat{A} & \hat{B} \\ \hat{C} & \hat{D} \end{bmatrix}, \ U(t) = \begin{bmatrix} \hat{x}(t) \\ u(t) \end{bmatrix}$$

and

$$V(t) = \begin{bmatrix} w(t) \\ w(t) \end{bmatrix}$$

indicates possible noise $w(t)$ due to the reconstruction of the state vector $x(t)$ and the similar additive noise $v(t)$ on the measured step response output $y(t)$. Combining all data for $t = 1, \ldots, N$ in a single matrix representation

$$\mathbf{Y} = \Theta \mathbf{U} + \mathbf{V}, \ \mathbf{Y} = \begin{bmatrix} Y(0) & Y(1) & \cdots & Y(N) \end{bmatrix}, \ \mathbf{U} = \begin{bmatrix} U(0) & U(1) & \cdots & U(N) \end{bmatrix} \tag{12}$$

shows that the state space matrices in Θ can be updated via a standard least-squares solution

$$\hat{\Theta}_{LS}^N = \frac{1}{N} \mathbf{Y}\mathbf{U}^T [\frac{1}{N} \mathbf{U}\mathbf{U}^T]^{-1} \tag{13}$$

provided $\mathbf{U}$ has full row rank. The condition of a full row rank $\mathbf{U}$ is related to the level of excitation the input signal $\{u(t)\}$ and is trivially satisfied for pulse or broadband excitation input signals.

It should be noted that the parameter estimate $\hat{\Theta}_{LS}^{N}$ in (13) can be used to re-estimate all the state space matrices. Obviously, with $\hat{A}$, $\hat{B}$ and $\hat{C}$ already available from the realization algorithm, one can simply compute the matrix $\hat{D}$ only, by choosing

$$Y(t) = \left[\begin{array}{c} y(t) - \hat{C}\hat{x}(t) \end{array}\right], \; \Theta = \left[\begin{array}{c} \hat{D} \end{array}\right], \; U(t) = \left[\begin{array}{c} u(t) \end{array}\right]$$

and combining all data for $t = 1, \ldots, N$ in same matrix representation as given in (12). If the system $G(q)$ is known to have at least one step time delay, the matrix $D = 0$ and the additional computation of $\hat{D}$ can be avoided by setting $\hat{D} = 0$. However, it is more advantageous to remove any delays from the input/output data and estimate a state space realization with a non-zero $\hat{D}$ to avoid the additional estimation of poles at zero in $\hat{A}$ due to any (known) time delays in the system $G(q)$.[6]

The additional least-squares estimation makes the estimation of the feedthrough matrix $\hat{D}$ less sensitive to noise. Let

$$\bar{y}(t) = C(qI - A)^{-1}Bu(t) \;\text{ and }\; \hat{y}(t) = \hat{C}(qI - \hat{A})^{-1}\hat{B}u(t)$$

and assume a consistent estimate of the state matrices (up to a singularity transformation), making

$$\lim_{N\to\infty} \hat{y}(t) = \bar{y}(t) \text{ w.p. } 1$$

then in case

$$\lim_{N\to\infty} \frac{1}{N}\mathbf{V}\mathbf{U}^T = 0 \tag{14}$$

a consistent estimate of the feedthrough matrix D is obtained

$$\lim_{N\to\infty} \hat{D} = D \text{ w.p. } 1$$

in the presence of a colored noise $\mathbf{V}$. The condition (14) is equivalent to the condition that the input $u(t)$ is uncorrelated with the noise $v(t)$ on the on the output $y(t)$. This condition can be satisfied asymptotically as $N \to \infty$ provided experiments are done in a way such that the input excitation is uncorrelated with measurement noise.

VI. Application to F/A-18AAW Model Aeroelastic Model

To illustrate the power of this realization method, the procedure is used to model the (poorly) damped resonance modes in the F/A-18 AAW aeroelastic model at a speed of Mach 0.90 and altitude of 15kft. The application of a step $u(t)$ on the Collective Leading Edge Flaperon was simulated and 1000 data points sampled at 200Hz (5 seconds of data) of the $y_i(t) = N_{ZKM023R}(t)$ (body normal acceleration at the right wing) were used to construct the 499×500 matrix R for the realization algorithm.

For the Mach 0.9 and 15kft condition, the singular value decomposition gives rise to a simple 9th-order model, $\hat{R}(q)$, for the map from $u(t)$ to $y_i(t)$. Although the 9th-order model is a simplication of the actual non-linear aeroelastic model used to generate the data, such simple linear models based on experimental data can accurately predict the main resonance modes and damping of the structure in the presense of small perturbations.[22] The measured step response (simulated with the F/A-18AAW aeroelastic model) and simulated step response (with the 9th order closed-loop model) show excellent agreement in Figure 3(a). The estimation of the poorly-damped resonance modes is also confirmed by the Bode plot of the 9th order model $\hat{R}_i(q)$ depicted in Figure 3(b).

To illustrate that the proposed step-based identification method also performs well in the presense of a poor signal-to-noise ratio, step-based simulation were performed on the F/A-18 AAW aeroelastic model in the presence of (random) gust disturbances.[23] Simulating the model at the same flight condition of Mach 0.90 and altitude of 15kft and in the presense of gust disturbances, the identification algorithm still captures the main resonance modes of the structure based on step-response excitation of the Collective Leading Edge Flaperon and measurements of the body normal acceleration at the right wing. The results of the measured signals and simulated response by the 9th-order linear model has been depicted in Figure 4. Again, the estimation of the poorly-damped resonance modes is also confirmed by the Bode plot of the 9th-order model $\hat{R}(q)$ depicted in Figure 4(b).

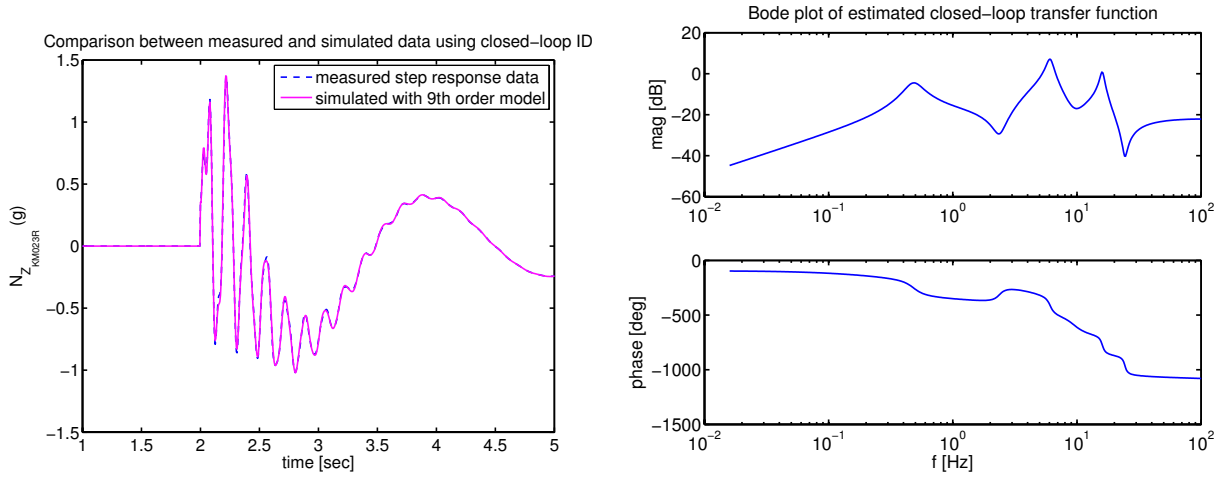

(a) Step Response

(b) Bode Plot of 9th order model $\hat{R}(q)$

Figure 3. Result of step-based identification method on non-linear F/A-18AAW Model at M=0.90, H= 15Kft.

VII. Conclusions

Using simple step-based excitation signals that can be applied to any of the control surfaces, this paper formulates an realization-based identification method that allows one to model aerodynamic induced structural vibration modes with little user intervention. The proposed method is a modified version of the well-known realization algorithm that is extended to arbitrary input signals to formulate a discrete-time model directly on the basis of step-based experiments. Since the numerical implementation only requires a singular value decomposition and a standard least-quares estimation, robust numerical algorithms can be put in place to formulate a dynamical model with little or no user intervention.

The procedure is illustrated on time-domain data obtained from a high fidelity 6-DOF rigid-body simulation model of the F/A-18AAW aircraft coupled to an linear aeroelastic solver. Even in the presence of a significantly small signal-to-noise ratio due to possible gust disturbances, the porposed step-based realization algorithm is able to find the location of the main resonance modes and damping ratios of the aeroelastic system and model them into a relatively low-order linear state-space model. The model can be used to tune an aerservoelastic controller to dampen structural vibrations via the control surfaces or impose limitations on the flight envelope based on the estimated structural vibrations.

References

[1]Raveh, D., "Identification of CFD-Based Unsteady Aerodynamic Models for Aeroelastic Analysis," *44th AIAA/ASME/ASCE/AHS Structures, Structural Dynamics, and Materials Conference*, AIAA-2003-1407, Norfolk, VA, 2003.

[2]Lind, R., Prazenica, R. J., Brenner, M. J., and Baldelli, D. H., "Identifying Parameter-Dependent Volterra Kernels to Predict Aeroelastic Instabilities," *AIAA Journal*, Vol. 43, 2005, pp. 2496–2502.

[3]Baldelli, D., Lind, R., and Brenner, M., "Nonlinear Aeroelastic/Aeroservoelastic Modeling by Block-Oriented Identification," *Journal of Guidance, Control, and Dynamics*, Vol. 28, No. 5, Sept.-Oct. 2005, pp. 1056–1064.

[4]Lind, R. and Brenner, M., *Robust Aeroservoelastic Stability Analysis: Flight Test Applications*, Springer-Verlag, London, Great Britain, 1999.

[5]Bachelder, E., Klyde, D., Thompson, P., and Harris, C., "System Identification Methods for Improved Flutter Flight Test Techniques," *AIAA Atomospheric Flight Mechanics Conference and Exhibit*, AIAA-2004-5065, 2004.

[6]Ljung, L., *System Identification: Theory for the User*, Prentice-Hall, Englewood Cliffs, NJ, 1999.

[7]Klein, V. and Morelli, A. E., *Aircraft System Identification: Theory and Practice*, AIAA Education Series, American Institute of Aeronautics and Astronautics, Reston, VA 20191, 2006.

[8]Jategaonkar, R. V., *Flight Vehicle System Identification: A Time Domain Methodology*, Vol. 216, AIAA, (Progress in Astronautics and Aeronautics Series), 2006.

[9]Van Overschee, P. and De Moor, B., "N4SID: Subspace algorithms for the identification of combined deterministic-stochastic systems," *Automatica*, Vol. 30, No. 1, 1994, pp. 75–93.

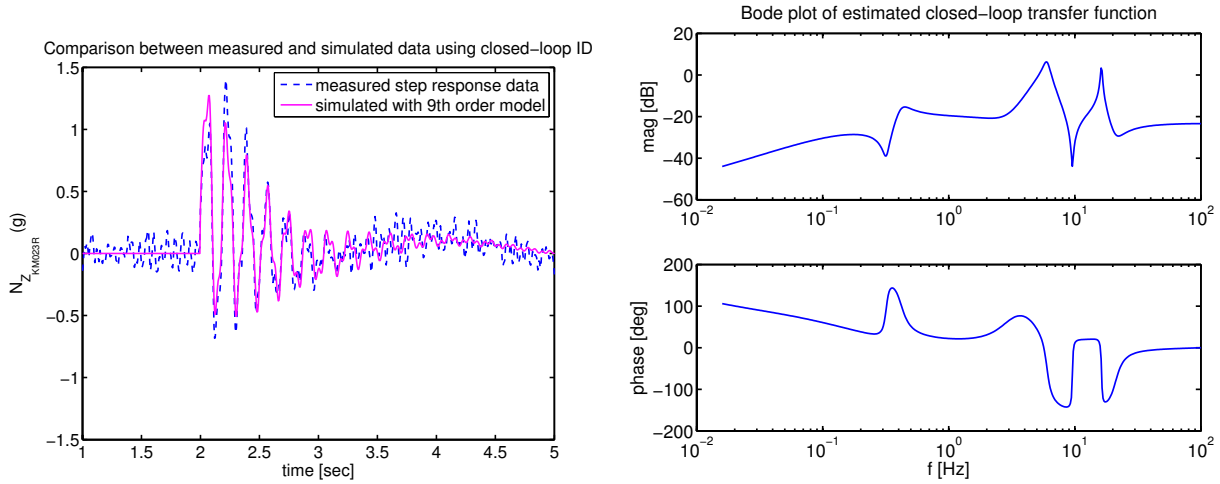

(a) Step Response

(b) Bode Plot of 9th order model $\hat{R}(q)$

Figure 4. Result of step-based identification method on non-linear F/A-18AAW Model at M=0.90, H= 15Kft with additional gust disturbances.

[10]Van Overschee, P. and De Moor, B., *Subspace Identification for Linear Systems: Theory, Implementation, Applications*, Kluwer Academic Publishers, 1996.

[11]Katayama, T., *Subspace Methods for System Identification*, Communications and Control Engineering, Springer-Verlag, 2005.

[12]Mehra, R., Arambel, P., Sampath, A., Prasanth, R., and Parham, T., "Self-Adaptive Notch Filter for the V-22 Flight Controls Using Stochastic Realization Algorithm (SRA)," Tech. Rep. N62269-96-C-0030, Scientific Systems Co., 1998.

[13]Juang, J. N. and Pappa, R. S., "An Eigensystem Realization Algorithm (ERA) for modal parameter identification and model reduction," *JPL Proc. of the Workshop on Identification and Control of Flexible Space Structures*, Vol. 3, April 1985, pp. 299–318.

[14]Plaetschke, E., Mulder, J. A., and Breeman, J. H., "Flight Test Results of Five Input Signals for Aircraft Parameter Identification," *Proc. Sixth IFAC Symposium on Identification and System Parameter Estimation*, Washington, DC, 1982, pp. 1149–1154.

[15]Morelli, E. A. and Klein, V., "Accuracy of Aerodynamic Model Parameters Estimated from Flight Test Data," *Journal Guidance, Control and Dynamics*, Vol. 20, No. 1, 1997, pp. 74–80.

[16]Chen, P., Baldelli, D., and Zeng, J., "Dynamic Flight Simulation (DFS) Tool for Nonlinear Flight Dynamic Simulation Including Aeroelastic Effects," *AIAA Guidance, Navigation and Control Conference and Exhibit*, AIAA-2008-6376, Honolulu, Hawaii, 2008.

[17]MathWorks, *Aerospace Blockset, User's Guide*, The MathWorks, Inc., Natick, MA 01760-2098, version 2 ed., March 2006.

[18]ZONA Technology, *ZAERO Version 7.4, Theoretical Manual*, 6 2006.

[19]Ho, B. L. and Kalman, R. E., "Effective construction of linear state-variable models from input/output functions," *Regelungstechnik*, Vol. 14, 1966, pp. 545–548.

[20]de Callafon, R. A., "Estimating parameters in a lumped parameter system with first principle modeling and dynamic experiments," *System Identification, 2003. 13th IFAC Symposium on*, 2003, pp. 1613–1618.

[21]Kung, S. Y., "A new identification and model redaction algorithm via singular value decomposition," *12th Asilomar Conference on Circuits, Systems and Computers*, 1978, pp. 705–714.

[22]Winther, B., Goggin, P. J., and Dykman, J. R., "Reduced-Order Dynamic Aeroelastic Model Development and Integration with Nonlinear Simulation," *Journal of Aircraft*, Vol. 37(5), 2005, pp. 833–839.

[23]Karpel, M., Moulin, B., and Chen, P., "Dynamic Response of Aeroservoelastic Systems to Gust Excitation," *Journal of Aircraft*, Vol. 42, 2005, pp. 1264–1272.